Inorganica Chimica Acta 407 (2013) 153–159

Contents lists available at ScienceDirect

Inorganica Chimica Acta

journal homepage: www.elsevier.com/locate/ica

Self-assembly of three cadmium(II) complexes based on 5-methylisophthalic acid and flexible bis(imidazole) ligands with different spacer lengths

Fei-Fei Li [a], Zhen-Zhen Shi [a,b], Lu-Fang Ma [b,*], Xiao-Jie Wu [b], Li-Ya Wang [b,c,*]

[a] Department of Physics and Chemistry, Henan Polytechnic University, Jiaozuo 454000, PR China
[b] College of Chemistry and Chemical Engineering, Luoyang Normal University, Luoyang 471022, PR China
[c] College of Chemistry and Pharmaceutical Engineering, Nanyang Normal University, Nanyang 473061, PR China

ARTICLE INFO

Article history:
Received 1 November 2012
Received in revised form 5 July 2013
Accepted 28 July 2013
Available online 3 August 2013

Keywords:
5-Methylisophthalic acid
Bis(imidazole) ligands
Spacer lengths

ABSTRACT

Three different cadmium(II) coordination polymers, $[Cd_2(mip)_2(1,2\text{-bie})]$ (**1**), [Cd(mip)(1,3-bip)] (**2**), $\{[Cd(mip)(1,4\text{-bib})(H_2O)]\cdot H_2O\}_2$ (**3**), where H_2mip = 5-methylisophthalic acid, 1,2-bie = 1,2-bis(imidazole)ethane, 1,3-bip = 1,3-bis(imidazole)propane and 1,4-bib = 1,4-bis(imidazole)butane, were synthesized under hydrothermal conditions. Their structures have been characterized by elemental analysis, IR and single-crystal X-ray crystallography. Complex **1** displays a 3D network with a (4,5)-connected $(4^2.7^4)(4^2.6^2.7^6)$ topology. Complex **2** features a 2D layer structure with a (3,5)-connected $(4^2.6)(4^2.6^7.8)$ topology. Complex **3** has two crystallographically distinct 2D (4,4) polymeric motifs, which are further extended by hydrogen-bonding interactions to form a 2D double layer. These structural analyses indicate that the flexible bis(imidazole) ligands with different spacer lengths play important roles in the formation of the final structures. In addition, the photoluminescent properties of **1**–**3** in the solid state have been investigated.

1. Introduction

The rational design, construction and characterization of new metal-organic frameworks (MOFs) is rapidly expanding in crystal engineering and materials chemistry, not only because of their potential applications in gas absorption [1–5], luminescence [6–8], magnetism [9–12], sensing [13–15] and so on, but also because of their fascinating structural diversities and intriguing topological features [16–18]. In principle, the control of coordination polymeric structure is complicated and still remains a major challenge in this field due to the fact that the self-assembly process influenced by many factors, such as the number, type and spatial disposition of coordination sites by organic ligands [19,20], the stereoelectronic preferences of the metal ions [21,22], metal–ligand ratio [23–25], solvent system [26,27], reaction temperature [28,29], pH value [30,31]. Up to now, the selection of suitable organic ligands is crucial for constructing extended coordination frameworks. Among them, flexible ligands can bend or rotate to adopt the appropriate conformation and hold the energetic minimum when coordinating to the metal centers, which often cause structural diversities [32].

Flexible bis(imidazole) ligands, such as 1,2-bis(imidazole)ethane (1,2-bie), 1,3-bis(imidazole)propane (1,3-bip), 1,4-bis(imidazole)butane (1,4-bib), 1,5-bis(imidazole)pentane (1,5-bip), 1,6-bis(imidazole)hexane (1,6-bih) and 1,4-bis(imidazol-1-ylmethyl)benzene (bix), with $-(CH_2)_n-$ ($n \geqslant 2$) spacers as their flexible backbones, have attracted considerable attention recently [33–37]. Their bis(imidazole) rings can freely twist around the $-(CH_2)_n-$ spacer group to meet the requirements of the coordination conformations (such as *cis-* and *trans-*) of metal atoms in the assembly process. Moreover, due to the presence of flexible $-(CH_2)_n-$, the bis(imidazole) ligands can act as bridges of different lengths to construct high dimensional frameworks and have different flexibility and conformational freedom, which may provide different capacities of spatial extension [31]. These features can induce the construction of diverse frameworks [38–43].

With this analysis in mind, we employed 5-methylisophthalic acid with Cd(II) salt and three bis(imidazole) ligands to give rise to three different structures, namely $[Cd_2(mip)_2(1,2\text{-bie})]$ **(1)**, [Cd(mip)(1,3-bip)] **(2)** and $\{[Cd(mip)(1,4\text{-bib})(H_2O)]\cdot H_2O\}_2$ **(3)**. Herein, we study syntheses, crystal structures and topological analysis of these three complexes. The influence of the spacer length in the flexible bis(imidazole) ligands on the structures of

---

* Corresponding authors at: College of Chemistry and Chemical Engineering, Luoyang Normal University, Luoyang 471022, PR China. Fax: +86 379 65526089.
E-mail addresses: mazhuxp@126.com (L.-F. Ma), wlya@lynu.edu.cn (L.-Y. Wang).

0020-1693/$ - see front matter © 2013 Elsevier B.V. All rights reserved.
http://dx.doi.org/10.1016/j.ica.2013.07.053

these complexes were also discussed. In addition, the photoluminescent properties of **1**–**3** in the solid state were also investigated.

2. Experimental

2.1. Materials and general methods

All chemicals purchased were used as received without further purification. All the products were highly stable in air at ambient conditions. Elemental analyses for carbon, hydrogen and nitrogen were performed on a Thermo Science Flash 2000 elemental analyzer. The infrared spectra (4000–600 cm^{-1}) were recorded on a NICOLET 6700 FT-IR spectrometer. Fluorescent analyses were performed on a Hitachi F-4500 analyzer.

2.2. Synthesis

2.2.1. Synthesis of [$Cd_2(mip)_2(1,2\text{-bie})$] (**1**)

A mixture of 5-methylisophthalic acid (18.0 mg, 0.1 mmol), 1,2-bie (16.2 mg, 0.1 mmol), $Cd(OAc)_2 \cdot 2H_2O$ (26.6 mg, 0.1 mmol), and KOH (5.6 mg, 0.1 mmol) were added to water (12 mL) in a 25 mL Teflon-lined stainless steel vessel. The mixture was heated at 413 K for 3 d, and then slowly cooled down to room temperature. Colorless block crystals of **1** were obtained. Yield: 17.5 mg, 47% (Based on Cd). *Anal.* Calc. for $C_{26}H_{22}Cd_2N_4O_8$: C, 41.83; H, 2.97; N, 7.51. Found: C, 41.78; H, 2.79; N, 7.64%. IR (cm^{-1}): 3131 m, 1608 m, 1541 s, 1412 m, 1352 s, 1243 m, 1096 m, 771 s, 731 s, 653 s.

2.2.2. Synthesis of [Cd(mip)(1,3-bip)] (**2**)

The reaction condition is similar to those described in **1** except that 1,2-bie was replaced by 1,3-bip (17.6 mg, 0.1 mmol). Colorless block crystals of **2** were obtained. Yield: 19.6 mg, 42% (Based on Cd). *Anal.* Calc. for $C_{18}H_{18}CdN_4O_4$: C, 46.32; H, 3.89; N, 12.00. Found: C, 46.28; H, 3.93; N, 11.96%. IR (cm^{-1}): 3484 m, 3118 m, 1615 m, 1546 s, 1370 s, 1090 s, 780 s, 730 s, 659 s.

2.2.3. Synthesis of {[Cd(mip)(1,4-bib)(H_2O)]·H_2O}$_2$ (**3**)

The reaction condition is similar to those described in **1** except that 1,2-bie was replaced by 1,4-bib (19.0 mg, 0.1 mmol). Colorless block crystals of **3** were obtained. Yield: 23.3 mg, 45% (Based on Cd). *Anal.* Calc. for $C_{38}H_{48}Cd_2N_8O_{12}$: C, 44.16; H, 4.68; N, 12.84. Found: C, 44.23; H, 4.78; N, 12.77%. IR (cm^{-1}): 3446 m, 3128 m, 2591 m, 1548 s, 1439 s, 1369 s, 1111 s, 774 s, 730 s, 657 s.

2.3. X-ray crystallographic data collection and structural determination

The crystallographic diffraction data for **1**–**3** were collected on a Bruker SMART APEX CCD diffractometer with graphite-monochromated Mo Kα radiation ($\lambda = 0.71073$ Å) at room temperature using the φ/ω scanning technique. All the structures were solved using direct methods and successive Fourier difference synthesis, and refined using the full-matrix least-squares method on F^2 with anisotropic thermal parameters for all non-hydrogen atoms using SHELXS-97 [44]. An empirical absorption correction was applied using the SADABS program [45]. The hydrogen atoms were placed in calculated positions and refined using a riding on attached atoms model with isotropic thermal parameters 1.2 times those of their carrier atoms. Corrections for L_p factors were applied and all non-hydrogen atoms were refined with anisotropic thermal parameters. Basic information pertaining to crystal parameters and structure refinements are summarized in Table 1. Selected bond lengths and angles for **1**–**3** are listed in Table S1, hydrogen bonding distance and angle data for **3** are listed in Table S2, shown in Supporting Information.

3. Results and discussion

3.1. Description of crystal structures

3.1.1. [$Cd_2(mip)_2(1,2\text{-bie})$] (**1**)

X-ray single crystal structure analysis reveals that the asymmetric unit of **1** consists of one crystallographically independent Cd(II), one mip anion, and half of a 1,2-bie molecule. As shown in Fig. 1(a), the Cd(II) ion is six-coordinated by one nitrogen atom of a 1,2-bie molecule and five carboxylate oxygen atoms from four separate mip ligands. The Cd–N bond length is 2.257(3) Å, and the Cd–O bond lengths are in the range of 2.291(2)–2.518(2) Å, respectively. Both of the carboxylate groups of mip are deprotonated, in agreement with the IR data in which no characteristic absorption bands of the –COOH group at 1700–1750 cm^{-1} are observed. The carboxylate groups of mip adopt μ_4-κ: O, O, O′, O″, O‴ coordination modes (Scheme 1(a)), linking the Cd atoms to result in an infinite 1D chain with the adjacent Cd···Cd distances of 3.8294(4) and 3.8796(4) Å along the *c* axis (see Fig. 1(b)). These chains are parallel to each other and are cross-linked by mip linkages to form a 3D framework with two kinds of channels (Fig. S1). The $-CH_3$ groups of the mip ligands protrude inside the voids of one type of channel and the other type of channel encapsulates *gauche* 1,2-bie ligands, which are bonded with Cd atoms through Cd–N coordination bonds (Fig. 1(c)). The 1,2-bie ligand adopts a *trans* conformation with a dihedral angle between two imidazole rings of 72.23°.

Analysis of the network topology of **1** reveals that each mip ligand acts as a 4-connected node, and Cd atom plays a 5-connected role. Thus, a (4,5)-connected 3D array with the Schläfli symbol of $(4^2.7^4)$ $(4^2.6^2.7^6)$ is formed (see Fig. 1(d)).

When 5-methoxyisophthalic acid (CH_3O-H_2ip) is selected as starting materials, {[Cd(CH_3O-ip)(1,2-bie)$_{0.5}$(H_2O)$_2$]·H_2O}$_n$ (**4**) [46] was obtained. **4** exhibits a 1D ladder-like chain, in which Cd(II) ion is seven-coordinated with a pentagonal bipyramid and CH_3O-H_2ip takes the bidentate-chelating coordination mode to bridge the neighboring Cd(II) ions.

3.1.2. [Cd(mip)(1,3-bip)] (**2**)

The asymmetric unit of **2** contains one mip anion, one Cd(II) ion and one 1,3-bip molecule. As illustrated in Fig. 2(a), Cd centre is six-coordinated with a distorted octahedral geometry by two *cis* nitrogen atoms from two 1,3-bip and four oxygen atoms from three mip. The apical positions are occupied by one nitrogen atom of 1,3-bip and one oxygen atom from mip with the N–Cd–O3 angle of 165.73(6)°. The Cd–N bond distances are 2.2471(16) and 2.3512(17) Å, and the Cd–O ones are in the range of 2.308(5)–2.524(4) Å, respectively. The carboxylate groups of mip adopt μ_3-κ: O, O′, O″, O‴ coordination modes (Scheme 1(b)) to coordinate with three Cd atoms. The adjacent Cd ions are bridged by mip ligands to form a 1D ribbon chain. The infinite chain comprises 8- and 16-membered rings with the Cd···Cd distances of 4.3275(3) and 8.0760(6) Å, respectively (Fig. 2(b)). Such 1D ribbon chains are further interlinked by 1,3-bip to form a 2D layer, in which the Cd···Cd distance across the 1,3-bip spacer is 11.4265(8) Å (Fig. 2(c)). Notably, the bidentate 1,3-bip ligand adopts the *cis*-conformation with a dihedral angle between two imidazole rings of 89.20° (see Fig. 2(c)).

From the topological perspective, the Cd(II) center and mip anion can be considered as a 5-connected node and a 3-connected node, respectively. Then the framework of **2** features a binodal (3,5)-connected network with a Schläfli symbol of $(4^2.6)(4^2.6^7.8)$ topology (see Fig. 2(d)).

When 5-methoxy isophthalic acid (CH_3O-H_2ip) are selected as starting material, {[Cd(CH_3O-ip)(1,3-bip)]·H_2O}$_n$ (**5**) [37] was obtained. **5** exhibits a similar binodal (3,5)-connected network as that

Table 1
Crystal and structural refinement data of **1**–**3**.

Complex	**1**	**2**	**3**
Empirical formula	$C_{26}H_{22}Cd_2N_4O_8$	$C_{18}H_{18}CdN_4O_4$	$C_{38}H_{48}Cd_2N_8O_{12}$
Formula weight	743.28	466.76	1033.64
T (K)	296(2)	296(2)	296(2)
Crystal size (mm)	0.34 × 0.30 × 0.29	0.35 × 0.21 × 0.19	0.21 × 0.08 × 0.05
Crystal system	tetragonal	monoclinic	orthorhombic
Space group	$P4_22_12$	$P2_1/n$	$Pna2_1$
a (Å)	18.2560(7)	10.3038(8)	24.608(3)
b (Å)	18.2560(7)	11.4265(8)	10.2320(12)
c (Å)	7.7060(6)	17.3227(13)	18.294(2)
β (°)	90	104.3150(10)	90
V (Å^3)	2568.3(2)	1976.2(3)	4606.3(9)
Z	4	4	4
D_{calc} (g/cm^3)	1.922	1.569	1.490
Absorption coefficient (mm^{-1})	1.715	1.135	0.988
$F(000)$	1464	936	2096
θ (°)	2.49–25.49	2.43–25.50	2.28–25.50
Limiting indices	$-22 \leqslant h \leqslant 22$, $-22 \leqslant k \leqslant 22$, $-9 \leqslant l \leqslant 9$	$-12 \leqslant h \leqslant 12$, $-13 \leqslant k \leqslant 13$, $-20 \leqslant l \leqslant 20$	$-29 \leqslant h \leqslant 29$, $-12 \leqslant k \leqslant 12$, $-22 \leqslant l \leqslant 22$
Reflections collected/unique	19626/2389	14723/3685	33940/8530
R_{int}	0.0196	0.0159	0.0945
Maximum and minimum transmission	0.6361, 0.5932	0.8133, 0.6921	0.8330, 0.3797
Data/restraints/parameters	2389/0/182	3685/0/245	8530/1/543
Goodness-of-fit (GOF) on F^2	1.077	1.061	1.002
R_1	0.0205	0.0184	0.0480
wR_2 [$I > 2\sigma(I)$]	0.0462	0.0476	0.0790
R_1 (all data)	0.0221	0.0207	0.0770
wR_2 (all data)	0.0471	0.0478	0.0872
$\Delta\rho_{max}$ and $\Delta\rho_{min}$ (e Å^{-3})	0.690, −0.271	0.329, −0.279	0.345, −0.571

in **2** except that Cd(II) ion takes a distorted trigonal bipyramidal geometry.

3.1.3. {[Cd(mip)(1,4-bib)(H_2O)]·H_2O}$_2$ (**3**)

Single-crystal X-ray characterization indicates that complex **3** comprises two crystallographically distinct 2D polymeric motifs, that is, two puckered (4,4) layers of [Cd(mip)(1,4-bib)(H_2O)]. As shown in Fig. 3(a), there are two crystallographic independent Cd(II) atoms, and both of which are six-coordinated with a distorted{CdN_2O_4} octahedral environment with three oxygen atoms from two different mip and a coordinated water molecule as well as two nitrogen atoms from two 1,4-bib. The apical positions are occupied by two nitrogen atoms with the N1#1–Cd1–N4 and N5–Cd2–N8#3 angles of 177.6(2) and 175.3(3)°. The Cd–N distances are 2.219(7) to 2.296(7) Å, and the Cd–O distances range from 2.308(5) to 2.524(4), respectively.

Both of the carboxylate groups of mip are deprotonated. As shown in Fig. 3(b), the carboxylate groups of mip adopt μ_2-κ: O, O′, O″ coordination modes (Scheme 1(c)) to link the adjacent Cd(II) ions to form a 1D linear chain in the two motifs. These 1D linear chains are further linked by μ_2-1,4-bib to generate two 2D frameworks parallel to the *ab* plane (Fig. 3(c) and (d)). The two crystallographically distinct 2D polymeric motifs are further packed into a 2D double layered structure by O–H···O hydrogen bonding interactions. Free water molecules are fixed by hydrogen bonding, located in the channels of the double layers (Fig. 3(e)). These hydrogen-bonding interactions bring further stability to the structure of **3**.

Three kinds of hydrogen bonds are present: (i) hydrogen bonding between coordinated water molecules and carboxylate oxygen atoms with O···O distances of 2.777(7) and 2.716(6) Å, respectively; (ii) hydrogen bonding between coordinated water molecule and free water molecules with O···O distances of 2.855(7) and 2.846(7) Å; (iii) hydrogen bonding between free water molecules and carboxylate oxygen atoms with O···O distances in the range of 2.722(11)–3.036(7) Å. The hydrogen-bonding metrics and bond parameters are shown in Table S2, Supporting Information.

When 5-nitroisophthalic acid (5-O_2N-H_2ip), 5-hydroxylisophthalic acid (5-HO-H_2ip) and Cd(II) salt are selected as starting materials, [Cd(1,4-bib)$_{0.5}$(5-O_2N-ip)(H_2O)]$_n$ (**6**), and {[Cd(1,4-bib)$_{0.5}$(5-HO-ip)](H_2O)}$_n$ (**7**) were generated [47]. In **6**, the 5-O_2N-H_2ip ligand links Cd(II) centers into a 1D double chain motif with alternating 8-membered and 16-membered rings. The 1,4-bib ligand as an *exo*-bidentate linkage extends the adjacent chain into a 2D layer. Complex **7** is a porous framework with guest water molecules, which arises from a 1D cadmium-carboxylate chain stretched by HO-ip and 1,4-bib. When 4,4′-bis(1-imidazolyl)bibenzene (bimb) and 1,4-bis(2-methylimidazol-1-yl)butane (bmib) are selected as starting materials [Cd(mip)(bimb)]$_n$ (**8**) [48] and [Cd(bmib)(mip)]$_n$ (**9**) [49] are synthesized. Complex **8** is a 3D framework in which 2D [Cd_4(mip)$_4$]$_n$ layers are interlinked by bimb. Complex **9** is a twofold interpenetrated 3D pcu topology containing binuclear Cd units.

3.2. Effect of bis(imidazole) ligands

To investigate the influence of the spacer length and flexibility of bis(imidazole) ligands on the complex structures, three typical bis(imidazole) ligands, 1,2-bie, 1,3-bip and 1,4-bib were used in terms of their differences in shape and flexibility. The synthetic strategy for the Cd(II)-H_2mip/ bis(imidazole) system is schematically depicted in Scheme 2.

From the structural descriptions above, we can see that the bis(imidazole) ligands can bend and rotate freely when

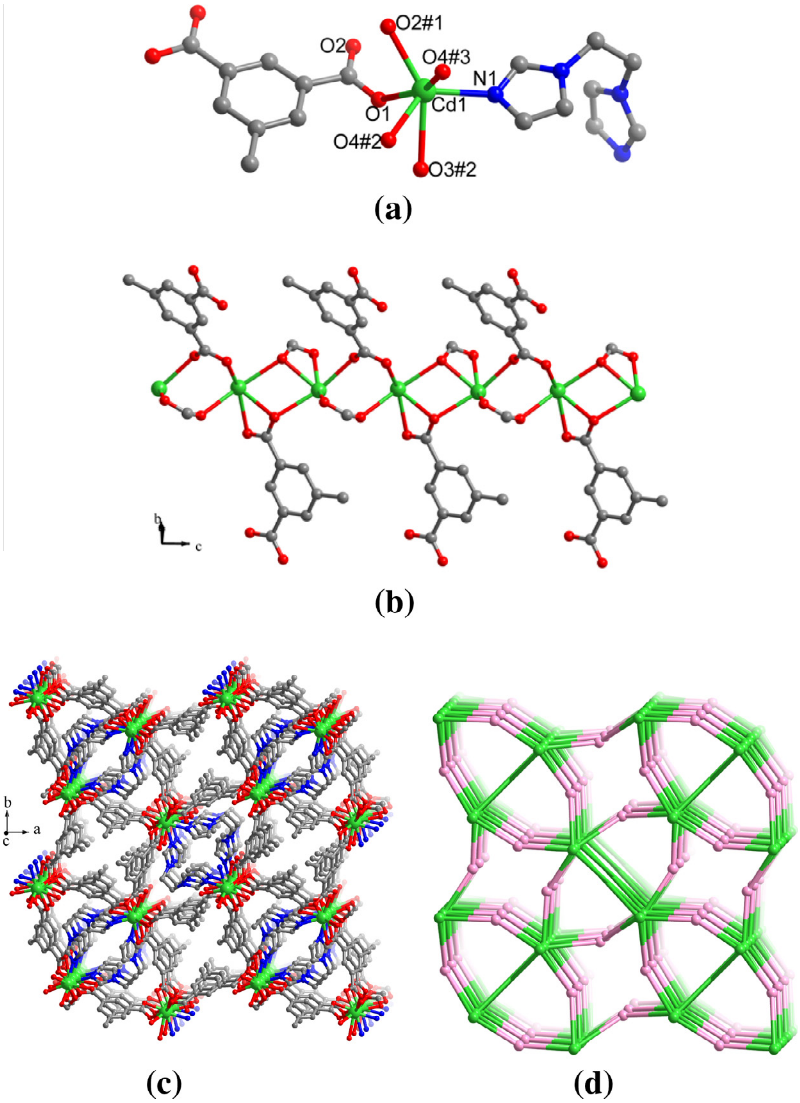

Fig. 1. (a) Coordination environments of the Cd(II) ion in **1**, hydrogen atoms are omitted for clarity. Symmetry codes: #1, x, y, $-z$; #2, $-x + 3/2$, $y - 1/2$, $z + 1/2$; #3, $-x + 3/2$, $y - 1/2$, $-z + 1/2$. (b) View of the 1D $[Cd_n(mip)_n]$ chain along the *c* axis in **1**. (c) Perspective view of the 3D coordination network along the *ab* plane in **1**. (d) Schematic view of the (4,5)-connected $(4^2.7^4)(4^2.6^2.7^6)$ topology in **1**. (green nodes for 5-connected Cd(II) and pink ones for mip). (For interpretation of the references to colour in this figure legend, the reader is referred to the web version of this article.)

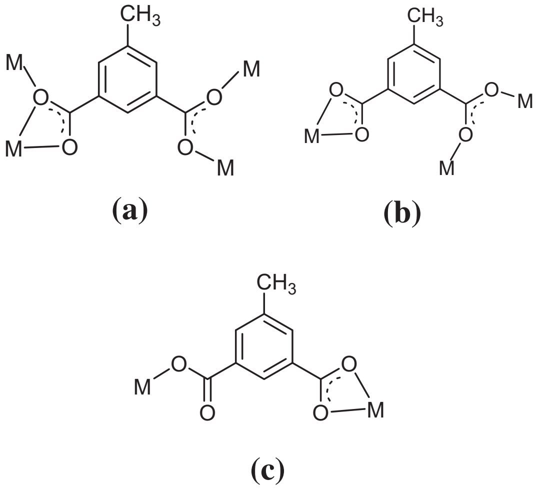

Scheme 1. Dicarboxylate coordination modes found in **1–3**.

coordinating to the central Cd ion due to the flexible nature of the spacers between the two imidazole rings. In **1**, the methylene groups of neutral 1,2-bie ligand display "***1***" conformations, with the distances between neighboring Cd centers linked by 1,2-bie being 9.4933(4) Å. In **2**, the methylene groups of neutral 1,3-bip ligand display "***3***" formed conformations, with the distances between neighbouring Cd centers linked by 1,3-bip being 11.4265(8) Å. In **3**, the neutral ligand is 1,4-bib, and the methylene groups display "***S***" conformations, with the distances in two similar polymeric motifs between neighboring Cd centers linked by 1,4-bib being 12.4611(16) and 12.3281(17) Å, respectively. The dihedral angles between the two imidazole rings are 72.23° for **1**, 89.20° for **2** and 12.09° for **3**, respectively.

As a result, a slight change in bis(imidazole) ligands has an impact on **1**–**3**. In **1**, the mip anions bridge the Cd(II) ions to form a 3D framework with two kinds of channels and *gauche* 1,2-bie ligands encapsulated inside the voids of one type of channel. In **2**, the mip anions bridge the Cd(II) ions to form a 1D ribbon $[Cd(mip)]_{2n}$ chains, which are further extended by the 1,3-bip ligands to generate a 2D layer with a $(4^2.6)(4^2.6^7.8)$ topology. Whereas, in **3**, the

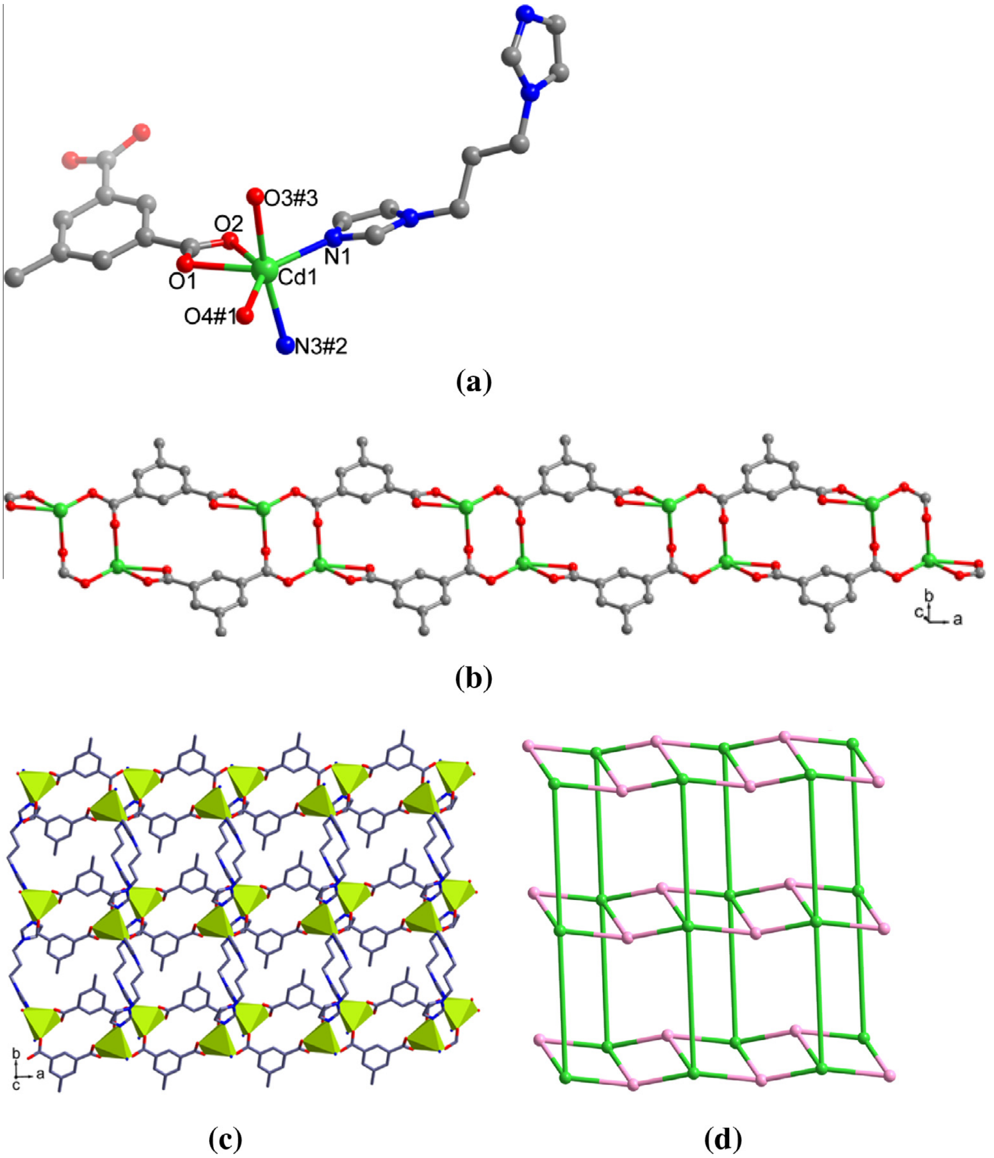

Fig. 2. (a) Coordination environments of the Cd(II) ion in **2**, hydrogen atoms are omitted for clarity. Symmetry codes: #1, $x + 1, y, z$; #2, $x, y + 1, z$; #3, $-x + 1, -y + 1, -z$. (b) View of the 1D $[Cd(mip)]_n$ chain in **2**. (c) Polyhedral View of the 2D layer in **2**. (d) Schematic view of the (3,5)-connected $(4^2.6)(4^2.6^7.8)$ topology in **2**. (green nodes for 5-connected Cd(II) and pink ones for mip). (For interpretation of the references to colour in this figure legend, the reader is referred to the web version of this article.)

$[Cd_n(mip)_n]$ chains are linked by 1,4-bib to generate two 2D frameworks with both (4,4) topologies. And these two crystallographically distinct 2D polymeric motifs are further packed into a 2D double layered structure by O-H···O hydrogen bonding interactions.

The spacer lengths of the bis(imidazole) ligands have also exerted a significant influence on the coordination modes of the carboxylate groups of mip ligands. There are three types of coordination modes in **1**–**3**: μ$_4$-κ: O, O, O′, O″, O‴ for **1**, μ$_3$-κ: O, O′, O″, O‴ for **2** and μ$_2$-κ: O, O′, O″ for **3**, respectively.

3.3. Photoluminescent properties

In the present paper, the photoluminescent properties of complexes **1**–**3** were studied in the solid state at room temperature, as depicted in Fig. 4. The emission spectra have broad peaks with maxima at 463 and 498 nm (λ_{ex} = 407 nm) for **1**, 435 nm (λ_{ex} = 316 nm) for **2**, 430 nm (λ_{ex} = 318 nm) for **3**, respectively. In order to understand the nature of such emission bands, the fluorescence properties of the free dicarboxylic acid ligands and Na salts for the dicarboxylate ligands were also measured, upon excitation at *ca.* 280 nm for H_2mip, and 300 nm for Na_2mip, which show the similar emissions at *ca.* 350 nm for H_2mip, and 328 nm for Na_2mip. In comparison with the free H_2mip and Na_2mip, the emission maxima of complexes **1**–**3** have changed and showed red shifts. Since the Cd(II) ions are difficult to oxidize or reduce, these bands may originate from the intraligand ($\pi \rightarrow \pi^*$) fluorescent emissions that are tuned by the metal–ligand interactions and deprotonated effect of the organic carboxylic ligands [50–52].

4. Conclusion

In summary, three new complexes based on 5-methylisophthalic acid and flexible bis(imidazole) ligands have been prepared under hydrothermal conditions. These three complexes are all based on the $[Cd_n(mip)_n]$ chains. However, by changing the spacer length of bis(imidazole)-based ligands ($-(CH_2)_2-$, $-(CH_2)_3-$ and $-(CH_2)_4-$), three complexes with different structures were constructed. **1**

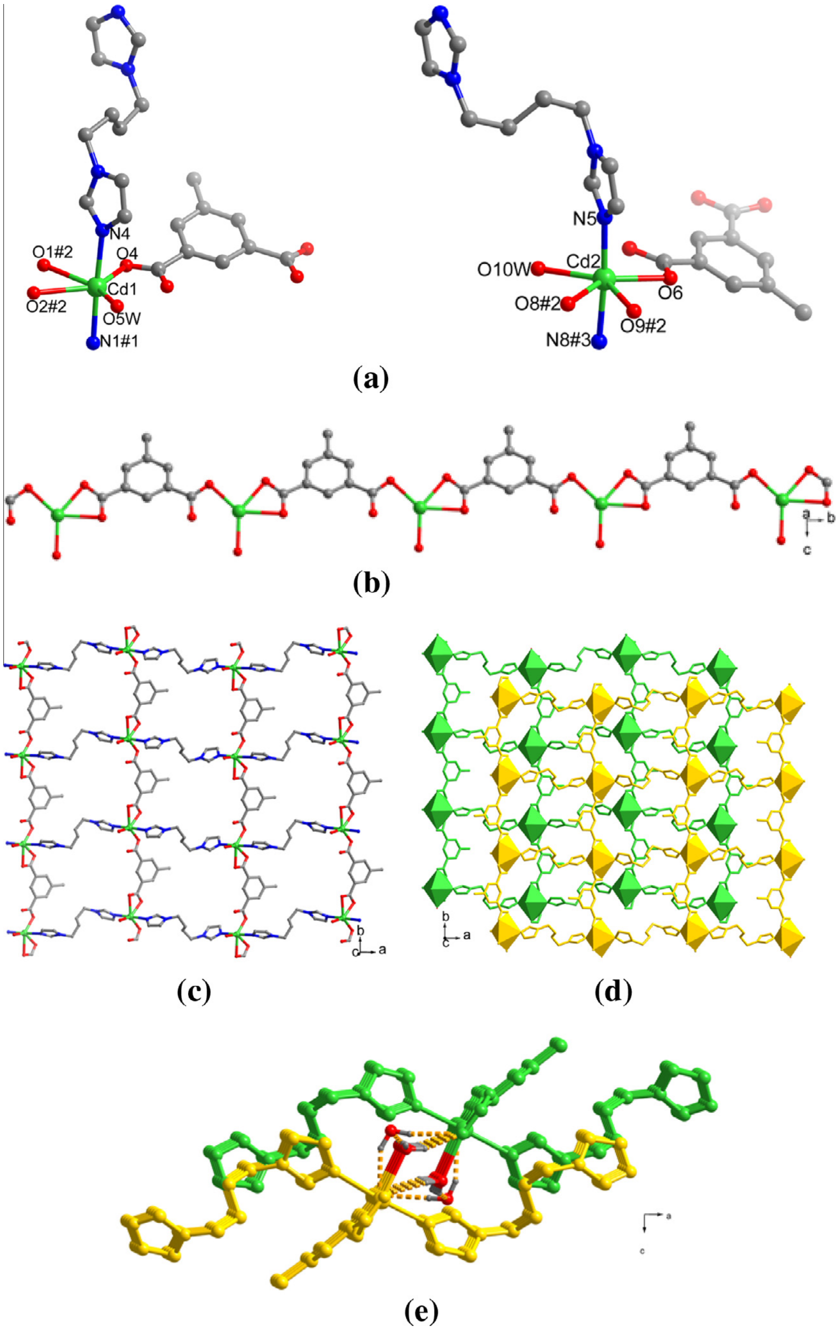

Fig. 3. (a) Coordination environments of the Cd1 and Cd2 ions in **3**, hydrogen atoms are omitted for clarity. Symmetry codes: #1, $x - 1/2, -y + 3/2, z$; #2, $x, y + 1, z$; #3, $x - 1/2, -y + 5/2, z$. (b) View of the 1D $[Cd(mip)]_{2n}$ chain in **3**. (c) Perspective view of the single 2D coordination network in **3**. (d) Polyhedral View of the 2D double layer along *c* axis in **3**. (e) View of the 2D double layer *via* hydrogen bonds in **3**. Hydrogen bonds are represented as light yellow dash line. (For interpretation of the references to colour in this figure legend, the reader is referred to the web version of this article.)

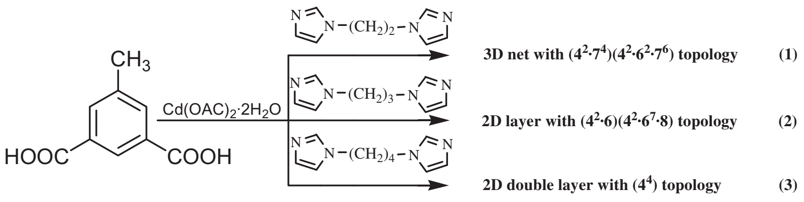

Scheme 2. Representation of synthesis of **1–3**.

displays a 3D structure with a $(4^2.7^4)$ $(4^2.6^2.7^6)$ topology. **2** shows a 2D layer with a $(4^2.6)$ $(4^2.6^7.8)$ topology, while **3** possesses a 2D double layer with a (4,4) topology. These structural analyses reveal that the spacer length and flexibility of bis(imidazole) ligands have

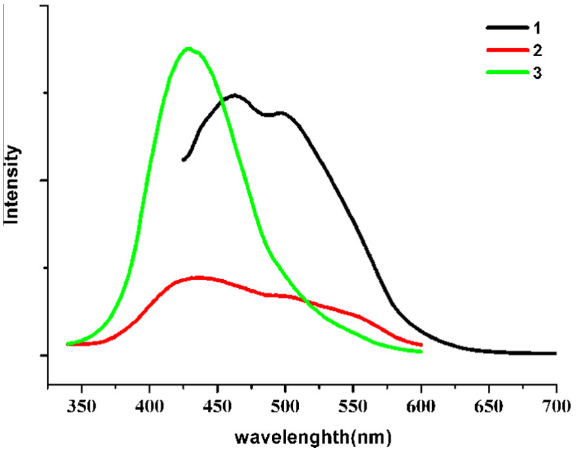

Fig. 4. The fluorescent emission spectra of **1–3** at room temperature.

important influences on the whole frameworks. Further experiments exploring the structural effects of methylene group substituents on bis(imidazole) or bis(triazole) coordination polymers, and any resulting changes in physicochemical properties, are underway in our laboratory.

Acknowledgment

This work was supported by the National Natural Science Foundation of China (21371089, 21073082 and 21271098), and sponsored by Program for New Century Excellent Talents in University (NCET-11-0947), Innovation Scientists and Technicians Troop Construction Projects of Henan Province (134100510011) and Program for Science & Technology Innovation Talents in Universities of Henan Province (2011HASTIT027).

Appendix A. Supplementary material

CCDC 876260–876262 contains the supplementary crystallographic data for complexes **1**–**3**. These data can be obtained free of charge from The Cambridge Crystallographic Data Centre via www.ccdc.cam.ac.uk/data_request/cif. Supplementary data associated with this article can be found, in the online version, at http://dx.doi.org/10.1016/j.ica.2013.07.053.

References

[1] W.M. Xuan, C.F. Zhu, Y. Liu, Y. Cui, Chem. Soc. Rev. 41 (2012) 1677.
[2] H.K. Chae, D.Y. Siberio-Pérez, J. Kim, Y.B. Go, M. Eddaoudi, A.J. Matzger, M. O'Keeffe, O.M. Yaghi, Nature 427 (2004) 523.
[3] M.P. Attfield, P. Cubillas, Dalton Trans. 41 (2012) 3869.
[4] G. Férey, C. Serre, Chem. Soc. Rev. 38 (2009) 1380.
[5] C.R. Tan, S.H. Yang, N.R. Champness, X. Lin, A.J. Blake, W. Lewis, M. Schröder, Chem. Commun. 47 (2011) 4487.
[6] J.J. Perry IV, P.L. Feng, S.T. Meek, K. Leong, F.P. Doty, M.D. Allendorf, J. Mater. Chem. 22 (2012) 10235.
[7] V. Wing-Wah, Chem. Commun. 47 (2011) 11579.
[8] M. Barwiolek, E. Szlyk, T.M. Muzioł, T. Lis, Dalton Trans. 40 (2011) 11012.
[9] E. Coronado, M. Giménez-Marqués, G.M. Espallargas, Inorg. Chem. 51 (2012) 4403.
[10] M. Wriedt, H.C.J. Zhou, Dalton Trans. 41 (2012) 4207.
[11] S.K. Langley, N.F. Chilton, B. Moubaraki, K.S. Murray, Dalton Trans. 41 (2012) 1033.
[12] A.M. Bryan, W.A. Merrill, W.M. Reiff, J.C. Fettinger, P.P. Power, Inorg. Chem. 51 (2012) 3366.
[13] B.V. Harbuzaru, A. Corma, F. Rey, J.L. Jorda, D. Ananias, L.D. Carlos, J. Rocha, Angew. Chem., Int. Ed. 48 (2009) 6476.
[14] Z.G. Xie, L.Q. Ma, J. Am. Chem. Soc. 132 (2010) 922.
[15] Z.Z. Lu, R. Zhang, Y.Z. Li, Z.J. Guo, H.G. Zheng, J. Am. Chem. Soc. 133 (2011) 4172.
[16] L.C. Gui, X.J. Wang, Q.L. Ni, M. Wang, F.P. Liang, H.H. Zou, J. Am. Chem. Soc. 134 (2012) 852.
[17] M.V. Kirillova, A.M. Kirillov, A.N.C. Martins, C. Graiff, A. Tiripicchio, A.J.L. Pombeiro, Inorg. Chem. 51 (2012) 5224.
[18] D.S. Li, P. Zhang, J. Zhao, Z.F. Fang, M. Du, K. Zou, Y.Q. Mu, Cryst. Growth Des. 12 (2012) 1697.
[19] A.M. Plonka, D. Banerjee, J.B. Parise, Cryst. Growth Des. 12 (2012) 2460.
[20] Q. Yang, X.F. Zhang, J.P. Zhao, B.W. Hu, X.H. Bu, Cryst. Growth Des. 11 (2011) 2839.
[21] R.F. Jin, S.Y. Yang, H.M. Li, L.S. Long, R.B. Huang, L.S. Zheng, CrystEngComm 14 (2012) 1301.
[22] Y.X. Tan, Y.P. He, J. Zhang, Chem. Commun. 47 (2011) 10647.
[23] F.H. Zhao, S. Jing, Y.X. Che, J.M. Zheng, CrystEngComm 14 (2012) 4478.
[24] Y. Liu, Y. Qi, Y.H. Su, F.H. Zhao, Y.X. Che, J.M. Zheng, CrystEngComm 12 (2010) 3283.
[25] X.P. Yang, R.A. Jones, M.M. Oye, M. Wiester, R.J. Lai, New J. Chem. 35 (2011) 310.
[26] Q.X. Yang, X.Q. Chen, Z.J. Chen, Y. Hao, Y.Z. Li, Q.Y. Lu, H.G. Zheng, Chem. Commun. 48 (2012) 10016.
[27] H.J. Hao, F.J. Liu, H.F. Su, Z.H. Wang, D.F. Wang, R.B. Huang, CrystEngComm 14 (2012) 6726.
[28] M. Chen, Y. Lu, J. Fan, G.C. Lv, Y. Zhao, Y. Zhang, W.Y. Sun, CrystEngComm 14 (2012) 2015.
[29] L.J. Dong, C.C. Zhao, X. Xu, Z.Y. Du, Y.R. Xie, J. Zhang, Cryst. Growth Des. 12 (2012) 2052.
[30] L.S. Long, CrystEngComm 12 (2010) 1354.
[31] H.Y. Liu, H. Wu, J. Yang, Y.Y. Liu, B. Liu, Y.Y. Liu, J.F. Ma, Cryst. Growth Des. 11 (2011) 2920.
[32] X.H. Zhou, X.D. Du, G.N. Li, J.L. Zuo, X.Z. You, Cryst. Growth Des. 9 (2009) 4487.
[33] Y. Yang, P. Du, J.F. Ma, W.Q. Kan, B. Liu, J. Yang, Cryst. Growth Des. 11 (2011) 5540.
[34] S.R. Zhu, H. Zhang, Y.M. Zhao, M. Shao, Z.X. Wang, M.X. Li, J. Mol. Struct. 892 (2008) 420.
[35] H. Qua, L. Qiu, X.K. Leng, M.M. Wang, S.M. Lan, L.L. Wen, D.F. Li, Inorg. Chem. Commun. 14 (2011) 1347.
[36] Y.P. Wu, D.S. Li, J. Zhao, Z.F. Fang, W.W. Dong, G.P. Yang, Y.Y. Wang, CrystEngComm 14 (2012) 4745.
[37] M.L. Han, J.G. Wang, L.F. Ma, H. Guo, L.Y. Wang, CrystEngComm 14 (2012) 2691.
[38] X.D. Du, C.H. Li, Y. Zhang, S. Liu, Y. Ma, X.Z. You, CrystEngComm 13 (2011) 2350.
[39] G.L. Wen, Y.Y. Wang, W.H. Zhang, C. Ren, R.T. Liu, Q.Z. Shi, CrystEngComm 12 (2010) 1238.
[40] X.L. Wang, D. Zhao, A.X. Tian, G.C. Liu, H.Y. Lin, Y.F. Wang, Q. Gao, X.J. Liu, N. Li, Inorg. Chim. Acta 388 (2012) 114.
[41] W.Q. Kan, Y.Y. Liu, J. Yang, Y.Y. Liu, J.F. Ma, CrystEngComm 13 (2011) 4256.
[42] X.J. Yang, H.X. Li, Z.L. Xu, H.Y. Li, Z.G. Ren, J.P. Lang, CrystEngComm 14 (2012) 1641.
[43] A.X. Tian, J. Ying, J. Peng, J.Q. Sha, H.J. Pang, P.P. Zhang, Y. Chen, M. Zhu, Z.M. Su, Cryst. Growth Des. 8 (2008) 3717.
[44] (a) G.M. Sheldrick, SHELXS-97, Program for Crystal Structure Solution, Göttingen University, Göttingen, Germany, 1997;
(b) G.M. Sheldrick, SHELXL-97, Program for Crystal Structure Refinement, Göttingen University, Göttingen, Germany, 1997;
(c) G.M. Sheldrick, Acta Crystallogr., Sect. A 64 (2008) 112.
[45] G.M. Sheldrick, SADABS. Program for Empirical Absorption Correction of Area Detector Data, Göttingen University, Germany, 2002.
[46] J.B. Guo, S.H. Li, Z. Kristallogr. NCS 227 (2012) 295.
[47] X.J. Li, R. Cao, W.H. Bi, Y.Q. Wang, Y.L. Wang, X. Li, Z.G. Guo, Cryst. Growth Des. 5 (2005) 1651.
[48] H.J. Cheng, H.X. Li, Z.G. Ren, C.N. Lv, J. Shi, J.P. Lang, CrystEngComm 14 (2012) 6064.
[49] F. Guo, J. Coord. Chem. 65 (2012) 4005.
[50] X.L. Wang, C. Qin, E.B. Wang, Y.G. Li, W. Hu, L. Xu, Chem. Commun. (2004) 378.
[51] C. Qin, X.L. Wang, L. Carlucci, M.L. Tong, E.B. Wang, C.W. Hu, L. Xu, Chem. Commun. (2004) 1876.
[52] H.Y. Bai, J.F. Ma, J. Yang, L.P. Zhang, J.C. Ma, Y.Y. Liu, Cryst. Growth Des. 10 (2010) 1946.